Predicted formation of superconducting platinum-hydride crystals under pressure in the presence of molecular hydrogen

Duck Young Kim[1], Ralph H. Scheicher[2], Chris J. Pickard[3], R. J. Needs[1],[*] and R. Ahuja[2,4][†]

[1] *Theory of Condensed Matter Group,*

Cavendish Laboratory, J J Thomson Avenue,

Cambridge CB3 0HE, United Kingdom

[2] *Condensed Matter Theory Group, Department of Physics and Astronomy,*

Uppsala University, P.O. Box 516, SE-751 20, Uppsala, Sweden

[3] *Department of Physics and Astronomy, University College London,*

Gower St, London WC1E 6BT, United Kingdom

[4] *Department of Materials and Engineering, Applied Materials Physics,*

Royal Institute of Technology (KTH), SE-100 44 Stockholm, Sweden

Abstract

Noble metals adopt close-packed structures at ambient pressure and rarely undergo structural transformation at high pressures. Platinum (Pt), in particular, is normally considered to be unreactive and is therefore not expected to form hydrides under pressure. We predict that platinum hydride (PtH) has a lower enthalpy than its constituents solid Pt and molecular hydrogen at pressures above 21.5 GPa. We have calculated structural phase transitions from tetragonal to hexagonal close-packed or face-centered cubic (fcc) PtH between 70 and 80 GPa. Linear response calculations indicate that PtH is a superconductor at these pressures with a critical temperature of about 10–25 K. These findings help to shed light on recent observations of pressure-induced metallization and superconductivity in hydrogen-rich materials. We show that formation of fcc metal hydrides under pressure is common among noble metal hydrides and examine the possibility of superconductivity in these materials.

PACS numbers: 63.20.kd, 74.25.Jb, 74.10.+v, 74.62.Fj

[*]Electronic address: rn11@cam.ac.uk

[†]Electronic address: rajeev.ahuja@fysik.uu.se

Pt maintains the face-centered cubic crystal structure up to at least 304 GPa [1], which covers most of the range currently accessible in static diamond anvil cell (DAC) experiments, and makes it suitable for use as a pressure standard [2, 3]. Pt is frequently used to form electrodes (which allow measurements of electrical resistance, the concentration of electrical carriers and the Hall mobility) and as a heat coupler. As a noble metal, Pt is fairly unreactive at ambient conditions, and this has generally been assumed also to hold at high pressures. However, chemical reactions of Pt with other materials present in the sample chamber can lead to the unexpected formation of new compounds as, for example, described by Gregoryanz *et al.* [4] who observed formation of Pt nitride when heating nitrogen with a piece of platinum.

The hydrogen-dense material silane (SiH_4) forms molecular crystals at low pressures. Two experimental studies of the metallization of SiH_4 under pressure have recently appeared [5, 6]. The first study [6] provided optical evidence for metallization of SiH_4 above 60 GPa. Remarkably, the second study by Eremets *et al.* [5] reported superconductivity of SiH_4 in the pressure range 60–150 GPa with a superconducting transition temperature as high as 17 K. These experimental findings have motivated a number of theoretical investigations of compressed SiH_4 [7–9] suggesting that metallization and/or superconductivity can be achieved under pressure, but a clear explanation of the observations has not yet been achieved. While the above two experimental studies [5, 6] reported metallization of SiH_4 above 60 GPa, whereas some other experiments claimed decomposition, amorphization, and the formation other metal-hydrogen alloys besides silane [10, 11]. This complexity itself is associated with hydrogen as being extremely light and mobile, as well as extraordinarily reactive. The properties of hydrogen are becoming drastically enhanced under high pressure and temperature, and make the interpretation of experimental data for hydrides [12–14] rather inconclusive.

Degtyareva *et al.* [11] have speculated that the formation of PtH under high pressures might explain some of the observations reported in Ref. 5, and they provided indirect evidence to support the hypothesis of PtH formation. Moreover, it appears likely that the silane in the experiments of Eremets *et al.* [5] partially decomposed, leading to release of hydrogen. Indeed SiH_4 is a metastable compound at low pressures which is thermodynamically unstable to decomposition into H_2 and Si [11], so that release of hydrogen might occur when the compression is sufficient to break bonds in the SiH_4 molecules. Released hydrogen may then have reacted with the Pt electrodes to form PtH as the pressure was further increased.

Confirming the formation of superconducting PtH at high pressures would change the inter-

pretation of the data of Eremets *et al.* [5], but would in no way diminish the importance of the experiments. In the new interpretation these experiments will have led to the discoveries of super-conducting PtH under pressure and a new insulating phase of SiH_4, and to the understanding that compressed SiH_4 is prone to decomposition. Indeed, Degtyareva *et al.* [11] have suggested that hydrogen release from SiH_4 at high pressures could be useful in synthesising metal hydrides.

The prevalence of DAC measurements and the steadily growing interest in high-pressure ex-perimental studies of metal hydrides raises the possibility of decomposition and hydrogen release in such experiments. Inadvertent and undetected formation of noble metal hydrides could lead to erroneous pressure estimates and other effects which could substantially alter the interpretation of the data. A careful investigation of the possibility of pressure-induced reactions between hydrogen and noble metals such as Pt is therefore very important and timely.

We have used *ab initio* random structure searching (AIRSS) to predict crystal structures of PtH under pressure [15]. This approach has been used to predict the structures of materials such as hydrogen [16], metal hydrides [17], transition metals [18], and molecular crystals [19–21]. In this study we have used the simplest version of the AIRSS technique in which an ensemble of structures is prepared by generating unit cells of random shapes with reasonable volumes into which the atoms are placed at random positions. The cell shapes and atomic positions are then relaxed to an enthalpy minimum at fixed pressure. We studied simulation cells containing 1, 2, 4, 6, and 8 formula units of PtH. We found three particularly low-enthalpy metallic structures of PtH (the corresponding space groups are given in parentheses): fcc ($Fm\bar{3}m$), hcp ($P6_3/mmc$), and tetragonal ($I\bar{4}m2$).

We have assumed that PtH forms in the 1:1 stoichiometry. The fcc structure was used for Pt and an hcp molecular form for hydrogen [16], in which the H_2 molecules are randomly oriented in space. The variation of the enthalpies H of the fcc, hcp, and tetragonal phases of PtH relative to that of $Pt + \frac{1}{2}H_2$ is given in Fig. 1, which shows that PtH is more stable at pressures above approxi-mately 20 GPa. We also calculated the dynamical stability of the PtH structures and evaluated their electron-phonon coupling (EPC) strengths, λ, in order to study the possibility of phonon-mediated superconductivity in PtH. Since the zero-point motion of the hydrogen nuclei is substantial, we have included effects from the zero-point enthalpy (ZPE) calculated within the quasiharmonic ap-proximation. For details of the computational methods we refer the reader to the supplementary material [22]. It should be noted that there are alternative ways of calculating the superconducting transition temperature T_c. In particular, there has recently been considerable progress within the

framework of density functional theory in developing truly *ab initio* quantitative predictions of T_c in the absence of adjustable parameters, which combine electron-phonon coupling and Coulomb interactions [23–28].
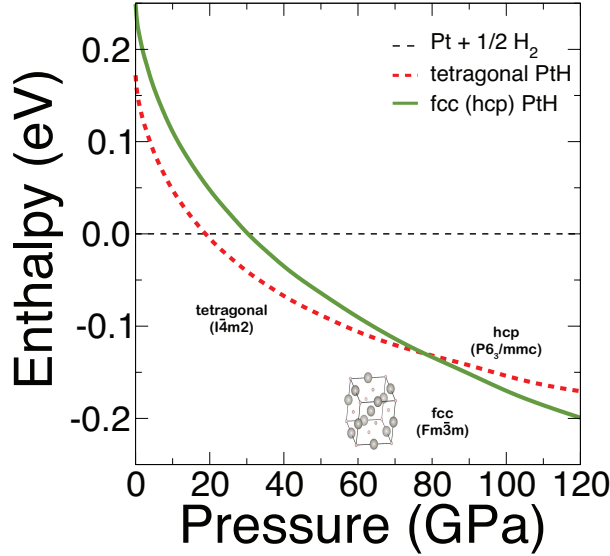

FIG. 1: (color online). Comparison of the enthalpies of Pt $+ \frac{1}{2}$H$_2$ and the tetragonal and fcc phases of PtH.

Figure 1 shows that it is thermodynamically favourable for tetragonal PtH to form from elemental Pt and H$_2$ above 18.7 GPa when the zero-point energy of the nuclei is neglected (above 21.5 GPa when the zero-point energy contribution is included; see the supplementary material [22]). Experimentally, a tetragonal PtH was observed at room temperature, 26 GPa on compression and 20 GPa on decompression [29]. We find a transition from tetragonal to hcp or fcc PtH between 70 and 80 GPa (Fig. 1). The fcc and hcp structures differ only in the stacking of layers, making them virtually degenerate in energy (to within a few meV per formula unit). Under pressure, a previous calculation using a simple model suggested that the site occupied by hydrogen in d-metal monohydrides tends to change from the tetrahedral to the octahedral site and that the hydride transforms into the hcp or fcc structure [30], in good agreement with our findings. In the present context it is more likely for fcc PtH to form, since the Pt atoms as the heavier host material are arranged in that structure prior to exposure to hydrogen. Experimentally hcp PtH not fcc PtH was observed and we therefore speculate that kinetics might favor a sequence of structural transformation from tetragonal PtH to hcp PtH.

Having established the likely formation of PtH from Pt and H$_2$ in the pressure range relevant for the experimental observations reported in Ref. 5, we evaluated the electron-phonon coupling

(EPC) strength in PtH to examine its potential for superconductivity, in a similar fashion to our studies of metal tri-hydrides [31, 34], as summarized in the supplementary material [22]. This study is crucial because the formation of superconducting SiH_4 was a central claim of Ref. 5, and perhaps superconducting PtH could provide an alternative explanation.
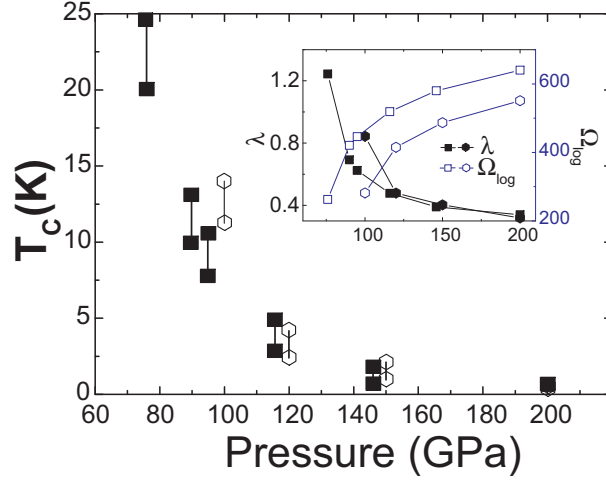

FIG. 2: (color online). Superconducting transition temperature T_c of PtH as a function of pressure. Filled squares and hollow hexagons show values of T_c for the fcc and hcp structures, respectively, with the higher T_c value at each pressure corresponding to the choice μ^*=0.10 and the lower T_c value to the choice μ^*=0.13. The inset displays the evolution with pressure of the electron-phonon coupling parameter, λ, and the asymptotic phonon momentum Ω_{log} (see the supplementary material [22]). The fcc phase is dynamically unstable below 77 GPa and the hcp phase is dynamically unstable below 100 GPa.

Papaconstantopoulos suggested that PtH could be superconducting under ambient conditions [35], but subsequent experiments found no evidence of PtH formation at low pressure [29, 41]. Tetragonal PtH becomes more stable than Pt + $\frac{1}{2}H_2$ above 20 GPa. We calculated the EPC of tetragonal PtH in the pressure range 20–60 GPa and found no significant coupling, so it is not likely that superconducting tetragonal PtH could exist. Figure 2 shows the variation of the calculated superconducting transition temperature T_c of PtH with pressure. In the whole pressure interval of 80–200 GPa we used a fixed value for the effective Coulomb interaction parameter $\mu^* = 0.13$, as has been common procedure [13, 36]. However, we also explored the effects on T_c of changing μ^* to 0.10 [12, 13]. With this, we have covered the two extreme choices of μ^*, resulting in corresponding high- and low-estimates of T_c (Fig. 2). It is worth noting that the value of μ^* may also be chosen to vary as a function of the electronic density of states at the Fermi level [39].

The highest value of T_c is found in the vicinity of the onset of dynamical stability of the structures, as expected for phonon-mediated superconductivity [31–33]. The fcc structure is dynamically stable above 77 GPa where it possesses the highest T_c of around 25 K. T_c decreases monotonically and quite rapidly as the pressure rises, as shown in Fig. 2, and reaches essentially zero around 140 GPa. The hcp structure is dynamically stable above 100 GPa (and is almost degenerate in enthalpy with fcc PtH) and its maximum T_c of around 15 K occurs at 100 GPa.
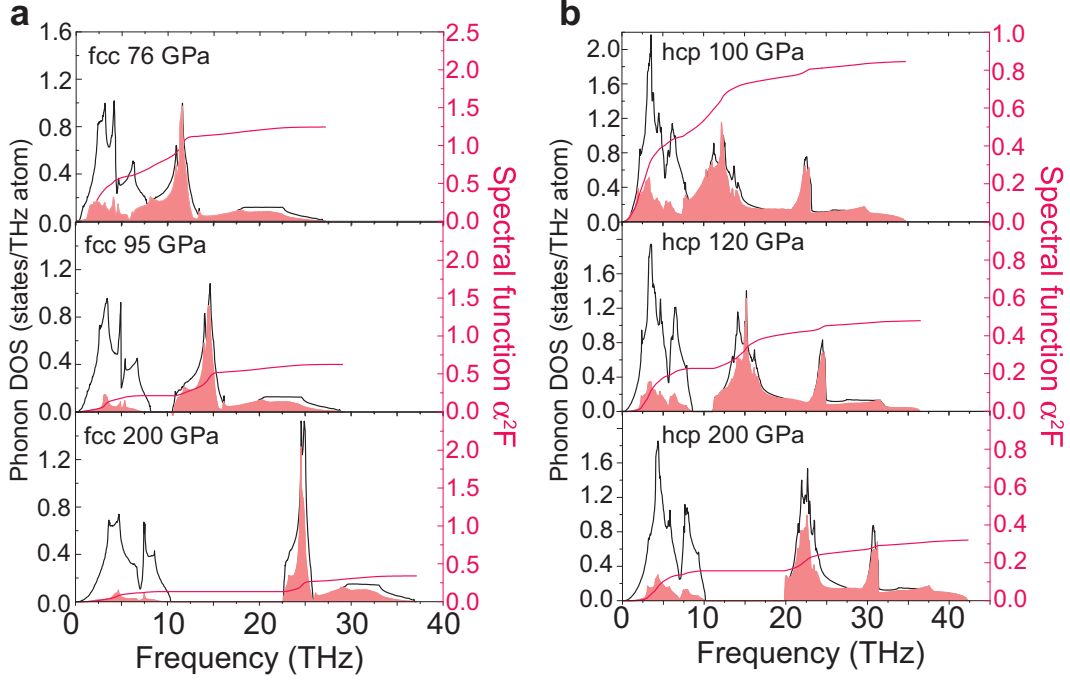

FIG. 3: (color online). Spectral function $\alpha^2 F$ (red shaded areas), the integral of the spectral function up to frequency ω ($\int_0^\omega \alpha^2 F(\omega')/\omega' \, d\omega'$) (red line), and the phonon density of states (solid black line) as a function of frequency at selected pressures for (a) fcc PtH and (b) hcp PtH.

Figure 3 shows the spectral function $\alpha^2 F$ and the phonon density of states (PhDOS) at different pressures for both fcc and hcp PtH. At the lowest pressure at which the fcc phase is stable (77 GPa), the Pt and H atoms both contribute to the EPC (Fig. 3a). With increasing pressure, the spectral function splits into high and low frequency bands as shown in the second and third panels of Fig. 3a, and only hydrogen vibrations contribute to the EPC in the higher pressure band. The situation is similar in the hcp phase (Fig. 3b), in the sense that the respective contributions to the EPC parameter λ from Pt and H are nearly the same as at lower pressures. With increasing pressure, the integrated λ decreases as the phonon frequencies increase. This behavior can be understood from Eq. 3 of the supplementary material [22], where it can be seen that the spectral function $\alpha^2 F$

is divided by the phonon frequencies.

Interestingly, Eremets *et al.* reported an apparent divergence in T_c between 80 and 100 GPa [5] which coincides with our calculated transition pressure between fcc and hcp PtH. These structural transformations are accompanied by softening of the acoustic branch modes which is a precursor of structural transformation. High-pressure experiments on PtH have been reported earlier [29], but since they were performed at room temperature, no information regarding possible superconductivity could be obtained. It would be very interesting to study compressed PtH at temperatures below 25 K to determine whether it is indeed superconducting.

At low pressures, fcc-Pt absorbs hydrogen and forms tetragonal PtH, which is a distortion of the fcc structure. Under pressure, the tetragonal PtH phase is restored to its original fcc structure or the similar close-packed hcp structure, which possess strong EPC and hence a high superconducting critical temperature. Such a structural transformation from a lower-symmetry phase to the fcc structure also applies to other hydrides formed by metals which are neighbors of Pt in the periodic table (referred to in the following as the Pt family of hydrides). We investigated the metals Rh, Pd, Ag, Ir, and Au, which all adopt the fcc structure at ambient pressure and have extremely small or zero superconducting T_c, and determined the onset pressure at which the corresponding fcc hydrides become dynamically stable. We find that fcc-RhH (lattice constant a = 4.02 Å) and fcc-PdH (a = 4.08 Å) are stable at almost ambient pressure, consistent with experimental observations [40, 42, 43, 45]. Also, our calculations are in good agreement with the measured lattice constants which were reported to be 4.01 Å at 3.8 GPa (hydrogen gas pressure) for fcc-RhH [42, 43] and 4.09 Å at ambient pressure for PdH [45]. The metal hydrides fcc-AgH (a = 4.00 Å) and fcc-IrH (a = 3.88 Å) are dynamically stable at 50 and 80 GPa, respectively. Dynamical stability of fcc-AuH (a = 3.80 Å) is achieved only above 220 GPa. We emphasize that other hydride structures besides fcc might be stable at lower pressures.

Similarly to PtH, the dynamical stability of other fcc-structure hydrides can be regarded as precursors for superconductivity, while lower symmetric structures might form at much lower pressures [44]. Figure 4 shows the calculated T_c at the onset of dynamical stability of the fcc structure in the Pt family of hydrides. PdH is calculated to possess a T_c of 20 K, which is compatible with experiments on non-stoichiometric PdH$_x$ which reported a T_c of 9 K [45], although we note that our results do not reproduce the observed isotope dependence of T_c in PdH/PdD [14]. We predict IrH to have a T_c of 7 K at 80 GPa. Remarkably, the T_c of fcc-AuH is estimated to be 21 K, however, it takes a very high pressure of 220 GPa to reach this superconducting state. As
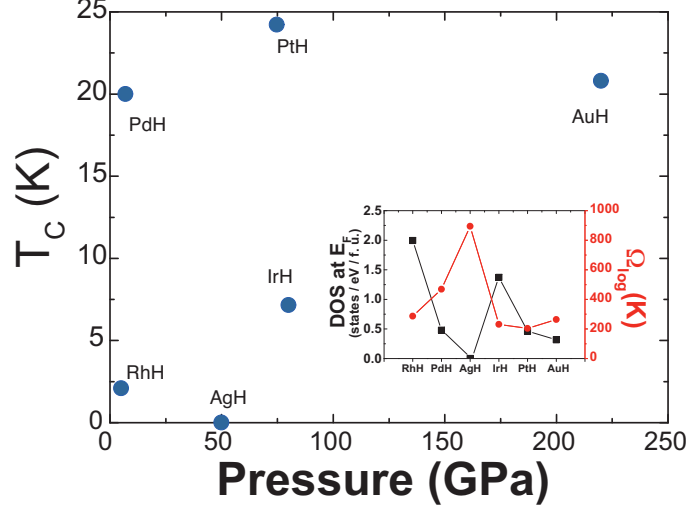
FIG. 4: (color online). Maximum T_c (calculated at the onset of dynamical stability of the fcc phase) for the metal hydrides RhH, PdH, AgH, IrH, PtH, and AuH. Note that the corresponding elemental metals in their fcc form all possess either extremely small T_c (Rh and Ir) or are not superconducting at all (Pd, Ag, Pt, and Au).

the pressure is increased, the T_c of all these fcc-hydrides will decrease, analogously to the case of PtH. We predict that AgH is not a superconductor, because the electronic density of states exhibits a small bandgap at the Fermi level. AgH does however possesses the highest Ω_{log}, and therefore, if electrons were to be donated in a complex alloy, this could lead to a good superconducting material, such as (PdAg)H$_x$, possessing a T_c of about 16 K [47]. RhH has a small T_c and it is worth note that no superconductivity of RhH has been detected at $T_c > 0.3$ K [48].

In conclusion, we have shown from first principles that formation of PtH from Pt and H$_2$ can occur under pressure. Based on the empirical Allen-Dynes equation (see supplementary material), the resulting product is predicted to be a superconductor. Throughout the studied pressure interval of 80–200 GPa, we used the effective Coulomb interaction parameter $\mu^* = 0.13$, a value which has often been used [36]. We did, however, consider the effect of changing μ^* to 0.10 on the predicted T_c. If our prediction concerning the formation of superconducting PtH at high pressures would be experimentally confirmed then this might lead to new interpretation of the data of Eremets *et al.* [5]. That work would mark the discovery of superconducting PtH under pressure and a new insulating phase of SiH$_4$, and to the understanding that compressed SiH$_4$ is prone to decomposition. We expect these findings to be relevant to recent observations of pressure-induced metallization

and superconductivity in hydrogen-rich materials. Indeed, our calculations show that the formation of superconducting fcc metal hydrides under pressure may be a common phenomenon among noble metal hydrides. The pressure-induced formation of PtH and of other noble metal hydrides, along with their associated superconductivity, represents an important aspect which should be considered in the interpretation of diamond anvil cell experiments whenever the corresponding metals and hydrogen are present, with the latter introduced either directly or entering via decomposition of hydrides.

---

[1] R. Ahuja, P. Söderlind, J. M. Wills, B. Johansson, and O. Eriksson, High Pressure Research **12**, 161 (1994).

[2] E. Y. Tonkov and E. G. Ponyatovsky, *Phase Transformations of Elements Under High Pressure* (CRC Press, Boca Raton, 2005), pp. 273–275.

[3] N. Holmes, J. Appl. Phys. **66**, 2962 (1989).

[4] E. Gregoryanz, C. Sanloup, M. Somayazulu, J. Badro, G. Fiquet, H.-k. Mao, and R. J. Hemley, Nature Mater. **3**, 294 (2004).

[5] M. I. Eremets, I. A. Trojan, S. A. Medvedev, J. S. Tse, and Y. Yao, Science **319**, 1506 (2008).

[6] X. J. Chen, V. V. Struzhkin, Y. Song, A. F. Goncharov, M. Ahart, Z. X. Liu, H.-k. Mao, and R. J. Hemley, Proc. Natl. Acad. Sci. U.S.A. **105**, 20 (2008).

[7] D. Y. Kim, R. H. Scheicher, S. Lebègue, J. Prasongkit, B. Arnaud, M. Alouani, and R. Ahuja, Proc. Natl. Acad. Sci. U.S.A. **105**, 16454 (2008).

[8] X.-J. Chen, J.-L. Wang, V. V. Struzhkin, H.-k. Mao, R. J. Hemley, and H.-Q. Lin, Phys. Rev. Lett. **101**, 077002 (2008).

[9] M. Martinez-Canales, A. R. Oganov, Y. Ma, Y. Yan, A. O. Lyakhov, and A. Bergara, Phys. Rev. Lett. **102**, 087005 (2009).

[10] C. Narayana, R. H. Greene, and A. L. Ruoff, J. Phys: Conf. Ser. **121**, 042019 (2008).

[11] O. Degtyareva, J. E. Proctor, C. L. Guillaume, E. Gregoryanz, and M. Hanfland, Solid State Communications **149**, 1583 (2009).

[12] B. Baranowski, Top. Appl. Phys. **29**, 157 (1978).

[13] B. Baranowski, S. Majchrzak, and T.B. Flanagan, J. Phys. F **1**, 258 (1971).

[14] E. G. Ponyatovskii, V. E. Antonov, and I. T. Belash, in "Problems in Solids State Physics", (A. M. Prokhorov and A. S. Prokhorov, Eds.), 109 MIR, Moscow (1984).

[15] C. J. Pickard and R. J. Needs, Phys. Rev. Lett. **97**, 045504 (2006).

[16] C. J. Pickard and R. J. Needs, Nature Phys. **3**, 473 (2007).

[17] C. J. Pickard and R. J. Needs, Phys. Rev. B **76**, 144114 (2007).

[18] C. J. Pickard and R. J. Needs, J. Phys.: Condens. Matter **21**, 452205 (2009).

[19] C. J. Pickard and R. J. Needs, Nature Mater. **7**, 775 (2008).

[20] A. D. Fortes, E. Suard, M.-H. Lemee-Cailleau, C. J. Pickard, and R. J. Needs, J. Am. Chem. Soc. **131**, 13508 (2009).

[21] P. Srepusharawoot, A. Blomqvist, C. M. Araújo, R. H. Scheicher, and R. Ahuja, Phys. Rev. B **82**, 125439 (2010).

[22] See supplementary material at `http://link.aps.org/supplemental/10.1103/PhysRevLett.xxx.xx` for details of the computational methods, crystal structures, and phonon enthalpy contributions.

[23] M. Lüders, M. A. L. Marques, N. N. Lathiotakis, A. Floris, G. Profeta, L. Fast, A. Continenza, S. Massidda, and E. K. U. Gross, Phys. Rev. B **72**, 024545 (2005).

[24] M. A. L. Marques, M. Lüders, N. N. Lathiotakis, G. Profeta, A. Floris, L. Fast, A. Continenza, E. K. U. Gross, and S. Massidda, Phys. Rev. B **72**, 024546 (2005).

[25] A. Floris, G. Profeta, N. N. Lathiotakis, M. Lüders, M. A. L. Marques, C. Franchini, E. K. U. Gross, A. Continenza, and S. Massidda, Phys. Rev. Lett. **94**, 037004 (2005).

[26] G. Profeta, C. Franchini, N. N. Lathiotakis, A. Floris, A. Sanna, M. A. L. Marques, M. Lüders, S. Massidda, E. K. U. Gross, and A. Continenza, Phys. Rev. Lett. **96**, 047003 (2006).

[27] A. Sanna, G. Profeta, A. Floris, A. Marini, E. K. U. Gross, and S. Massidda, Phys. Rev. B **75**, 020511 (2007).

[28] A. Floris, A. Sanna, S. Massidda, and E. K. U. Gross, Phys. Rev. B **75**, 054508 (2007).

[29] N. Hirao, F. Hiroshi, O. Yasuo, T. Kenichi, and K. Takumi, Acta Cryst. **64**, C609 (2008).

[30] V. A. Somenkov, V. P. Glazkov, A. V. Irodov, and S. Sh. Shilstein, J. Less-Common Metals **129**, 171 (1987).

[31] D. Y. Kim, R. H. Scheicher, H.-k. Mao, T. W. Kang, and R. Ahuja, Proc. Natl. Acad. Sci. U.S.A. **107**, 2793 (2010).

[32] Y. Yao, J. S. Tse, K. Tanaka, F. Marsiglio, and Y. Ma, Phys. Rev. B **79**, 054524 (2009).

[33] D. Erskine, P. Y. Yu, K. J. Chang, and M. L. Cohen, Phys. Rev. Lett. **57**, 2741 (1986).

[34] D. Y. Kim, R. H. Scheicher, and R. Ahuja, Phys. Rev. Lett. **103**, 077002 (2009).

[35] D. A. Papaconstantopoulos, J. Less-Common Metals **73**, 305 (1980).

[36] N. W. Ashcroft, Phys. Rev. Lett. **92**, 187002 (2004).

[37] W. L. McMillan, Phys. Rev. **167**, 331 (1968).

[38] P. B. Allen and R. C. Dynes, Phys. Rev. B **12**, 905 (1975).

[39] K. H. Bennemann and J. W. Garland, AIP Conference Proceedings **4**, 103 (1972).

[40] Y. Fukai, *Metal-hydrogen system* (Springer, Berlin and Heidelberg, 2003).

[41] A. Traverse, H. Bernas, J. Chaumont, L. Dumoulin, and M. Gupta, Solid State Commun. **40**, 725 (1981).

[42] M. Tkacz, J. Chem. Phys. **108**, 2084 (1998).

[43] V. E. Antonov, J. Alloys Compd. **330-332**, 110 (2002).

[44] V. E. Antonov, T. E. Antonova, I. T. Belash, A. E. Gorodezkii, and E. G. Ponyatovskii, Dokl. Acad. Nauk. SSSR **266**, 376 (1982).

[45] H. Hemmes, A. Driessen, R. Griessen, and M. Gupta, Phys. Rev. B **39**, 4110 (1989).

[46] B. Stritzker and W. Buckel, Z. Physik **257**, 1 (1972).

[47] W. Buckel and B. Stritzker, Phys. Lett. A **43**, 403 (1973).

[48] V. E. Antonov, I. T. Belash, O. V. Zharikov, and A. V. Palnichenko, Phys. Stat. Sol. **142**, K155 (1987).

Supplementary Material

"Formation and superconductivity of platinum hydride under pressure"

D. Y. Kim, R. H. Scheicher, C. J. Pickard, R. J. Needs, and R. Ahuja

A. Methods

Our results were obtained using density-functional-theory (DFT) methods [1, 2] and the generalized gradient approximation (GGA) of Perdew, Burke and Ernzerhof for the exchange-correlation functional [3, 4]. The structure searching was carried out with the CASTEP plane-wave code [5] and ultrasoft pseudopotentials [6]. For the searches we used a plane-wave basis-set cutoff of 550 eV and a Brillouin-zone integration grid of spacing $2\pi \times 0.07$ Å^{-1}. The structures of interest were further relaxed for enthalpy comparisons, which were done with the VASP code [7, 8] with the projector-augmented wave (PAW) approach [9]. A cutoff energy of 700 eV was found to produce converged results. The Monkhorst-Pack scheme [10] was used to generate the k-point grid meshes of $31 \times 31 \times 31$ for Pt and PtH (Γ-centered in the case of hcp-PtH). For calculations of solid hydrogen, a large supercell containing 36 H$_2$ molecules was used; therefore, the Brillouin-zone was only sampled at the Γ-point. Calculations of the phonon modes and frequencies were performed with density-functional perturbation theory using the QUANTUM ESPRESSO code [11]. The electronic orbitals were expanded in a plane-wave basis set with a kinetic energy cutoff of 60 Ry. The Brillouin zone (BZ) integrations in the electronic and phonon calculations were performed using Monkhorst-Pack meshes. We refer to meshes of k-points for electronic states and meshes of q-points for phonons. The EPC matrix elements were computed in the first BZ on a $8 \times 8 \times 8$ q-mesh ($8 \times 8 \times 4$ q-mesh) using individual EPC matrices obtained with a $24 \times 24 \times 24$ $(24 \times 24 \times 16)$ k-points mesh for fcc (hcp). Convergence tests of the EPC calculations were performed with up to $12 \times 12 \times 12$ q-meshes for fcc and $8 \times 8 \times 8$ q-meshes for hcp.

The total phonon zero-point energy was calculated as $E_{ph} = \frac{1}{2} \sum_i \hbar \omega_i$ over a range of volumes V, where $\hbar \omega_i$ are the individual phonon energies. We fitted the results to a polynomial and differentiated with respect to V to obtain the zero-point enthalpy as $H_{ph} = E_{ph} - V dE_{ph}/dV$.

T_c was calculated using the Allen-Dynes equation,[12]

$$T_c = \frac{\Omega_{log}}{1.2} \exp\left(-\frac{1.04(1+\lambda)}{\lambda - \mu^*(1 + 0.62\lambda)}\right), \tag{1}$$

12

with the standard value $\mu^* = 0.13$. The normalized weighting function of the Eliashberg theory [13] is

$$g(\omega) = \frac{2}{\lambda\omega}\alpha^2 F(\omega). \tag{2}$$

The parameter λ is a dimensionless measure of the strength of $\alpha^2 F$:

$$\lambda = 2 \int_0^\infty d\omega \, \alpha^2 F(\omega)/\omega, \tag{3}$$

and the logarithmic average frequency, Ω_{log} in units of K, is

$$\Omega_{log} = \exp\left(\int_0^\infty g(\omega) \ln\omega \, d\omega\right). \tag{4}$$

B.   Crystal structure details

tetragonal PtH at 46.6 GPa

lattice vectors:

$a = b = 3.422$ Å, $c = 2.782$ Å

atomic positions:

 Pt 1/2   0   3/4

 Pt   0   1/2 1/4

 H   0   0   0

 H 1/2 1/2 1/2

fcc PtH at 40.6 GPa

lattice vector:

$a = 2.843$ Å

atomic positions:

 Pt 1/2 1/2 1/2

 H   0   0   0

hcp PtH at 48.1 GPa

lattice vectors:

$a = 2.789$ Å, $c = 4.733$ Å

atomic positions:

 Pt 1/3 2/3 1/4

 Pt 2/3 1/3 3/4

 H   0   0   0

 H   0   0   1/2

C. Phonon enthalpy contribution

Figure 5 shows the effect of the nuclear zero-point enthalpy (ZPE) H_{ph}, as defined in the Methods section, on the formation pressure of PtH. The difference in total enthalpy between tetragonal PtH and Pt + $\frac{1}{2}$ H$_2$ is plotted. As can be seen, the inclusion of H_{ph} shifts the formation pressure up to 51.8 GPa, far beyond the 18.7 GPa obtained when the ZPE is neglected. Such a shift seems unreasonably high, and we therefore decided to calculate the effect of H_{ph} for a material with a well-established formation pressure.

PdH is known to form close to ambient pressure [14]. Figure 6 shows that the enthalpy comparison of PdH with Pd + $\frac{1}{2}$ H$_2$ yields a formation pressure in the vicinity of 0 GPa, actually slightly below it. However, once H_{ph} is included, the formation pressure shifts to 23 GPa (Fig. 6), in contradiction with experiment.

What is the source of this discrepancy? The zero-point enthalpy H_{ph} contributions from the metal and metal hydride can be rather precisely determined computationally, in particular because there is very little uncertainty about the slope dE_{ph}/dV, the phonon pressure term, which is multiplied by the volume and added to the phonon energy to yield the phonon enthalpy H_{ph}. For Pt and PtH, the phonon energy E_{ph} is found to depend linearly on the cell volume, and so dE_{ph}/dV remains virtually constant throughout the pressure range studied. The main uncertainty stems from the contribution to H_{ph} from H$_2$, a system which is notoriously difficult to describe properly within density functional theory at low pressures [15]. As a consequence, it is hard to determine the phonon energy E_{ph} accurately at low pressures, and furthermore, the non-linear dependence of E_{ph} on V in solid hydrogen (see Figure 7) prevents us from obtaining a reliable value of dE_{ph}/dV at lower pressure.

To correct for the error in E_{ph} and in the slope dE_{ph}/dV, we therefore determined a correction factor which multiplies H_{ph} for H$_2$, in order to recover the known formation pressure of PdH. Figure 6 shows the enthalpy when H_{ph} for H$_2$ is scaled by a factor of 3.3, which yields a reasonable formation pressure in the vicinity of 0 GPa.

Applying the same scaling correction to H_{ph} for H$_2$ in the enthalpy comparison for PtH (Fig. 8), we obtain a formation pressure of 21.5 GPa, corresponding to a much more reasonable shift of 2.8 GPa due to the effects of ZPE.
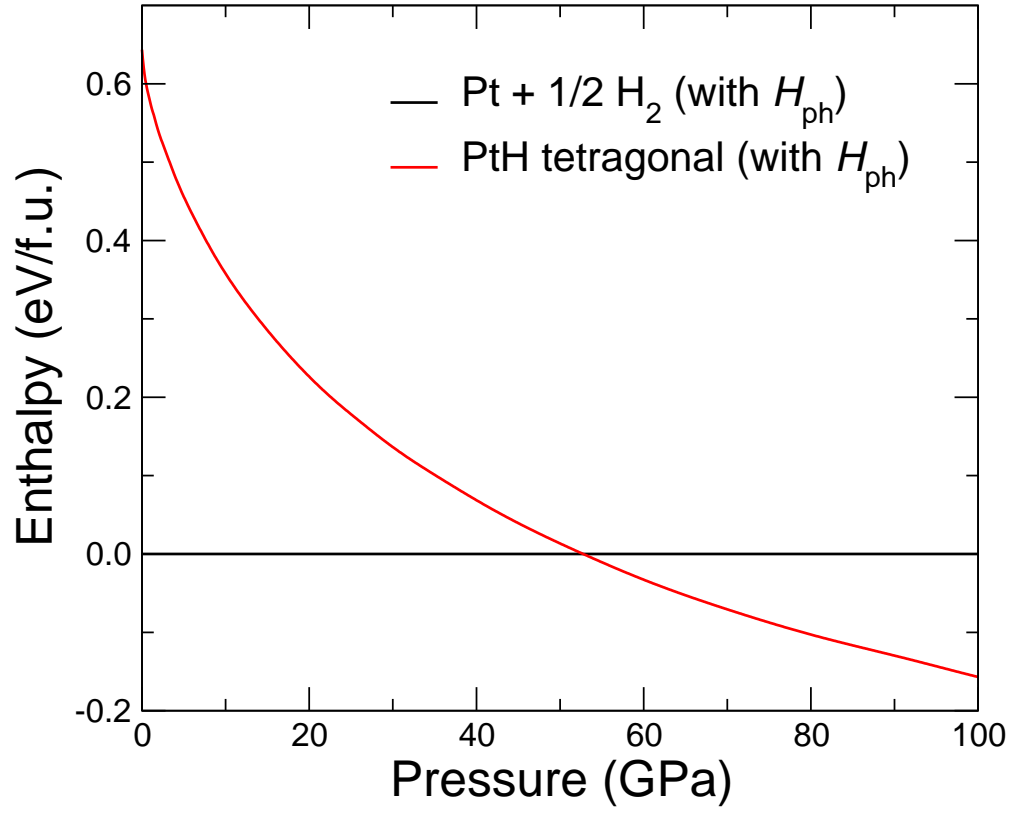
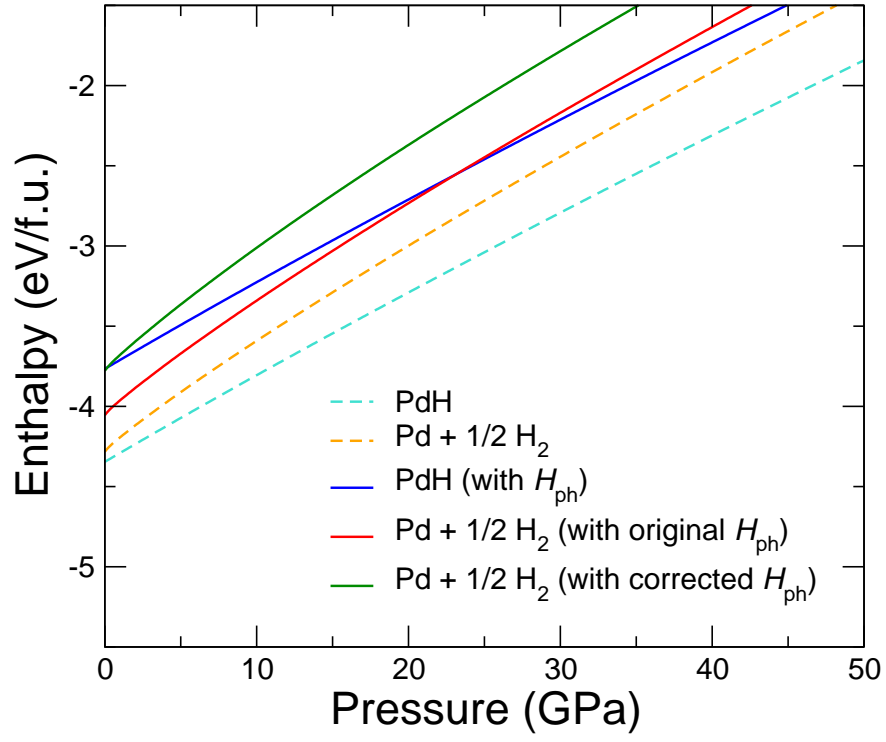FIG. 5: Comparison of the enthalpies of $Pt + \frac{1}{2} H_2$ and the tetragonal phase of PtH with H_{ph} included.

FIG. 6: Comparison of the enthalpies of Pd + $\frac{1}{2}$ H$_2$ and PdH without H_{ph}, with H_{ph}, and with the corrected H_{ph} contribution.
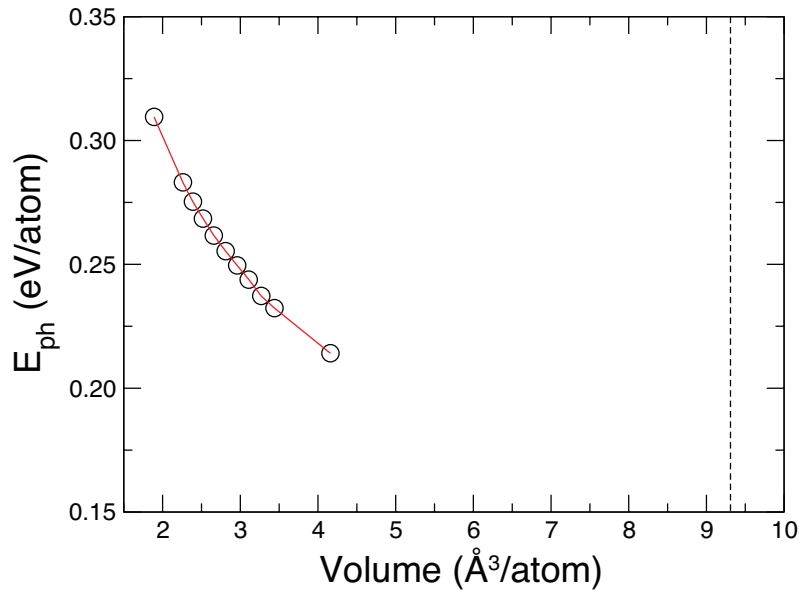
FIG. 7: E_{ph} for solid H_2 is plotted as a function of volume. The calculated data are shown as black circles. The connecting red lines are merely a guide to the eye. The vertical dashed line indicates the equilibrium volume of hydrogen at zero pressure.
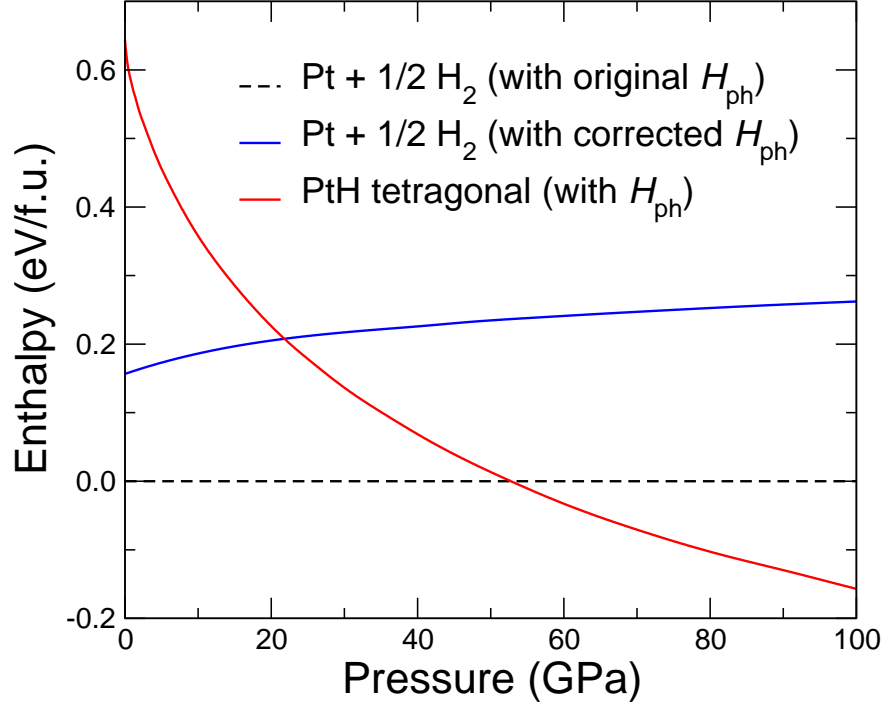
FIG. 8: Comparison of the enthalpies of Pt + $\frac{1}{2}$ H$_2$ and tetragonal-PtH, including the correction discussed in the text.

[1] P. Hohenberg and W. Kohn *Phys. Rev.* **136**, B864–B871 (1964).

[2] W. Kohn and L. J. Sham *Phys. Rev.* **140**, A1133–A1138 (1965).

[3] J. P. Perdew, J. A. Chevary, S. H. Vosko, K. A. Jackson, M. R. Pederson, D. J. Singh, and C. Fiolhais *Phys. Rev. B* **46**, 6671–6687 (1992).

[4] J. P. Perdew, K. Burke, and M. Ernzerhof *Phys. Rev. Lett.* **77** 3865–3868 (1996).

[5] S. J. Clark, S. J. *et al*. *Z. Kristallogr.* **220**, 567–570 (2005).

[6] D. Vanderbilt *Phys. Rev. B* **41**, 7892–7895 (1990).

[7] G. Kresse and J. Furthmüller *Phys. Rev. B* **54**, 11169–11186 (1996).

[8] G. Kresse and J. Furthmüller *Comput. Mater. Sci.* **6**, 15–50 (1996).

[9] P. E. Blöchl *Phys. Rev. B* **50** 17953–17979 (1994).

[10] H. J. Monkhorst, and J. D. Pack *Phys. Rev. B* **13**, 5188–5192 (1976).

[11] S. Baroni, S. de Gironcol, A. Dal Corso, and P. Giannozzi *Rev. Mod. Phys.* **73**, 515–562 (2001).

[12] P. B. Allen and R. C. Dynes *Phys. Rev. B* **12**, 905–922 (1975).

[13] W. L. McMillan *Phys. Rev.* **167**, 331–344 (1968).

[14] B. Stritzker and W. Buckel *Z. Physik* **257**, 1–8 (1972).

[15] D. M. Ceperley and B. J. Alder *Phys. Rev. B* **36**, 2092–2106 (1987).